



Syddansk Universitet

Organic nanofiber-loaded surface plasmon-polariton waveguides

Radko, Ilya; Fiutowski, Jacek; Tavares, Luciana ; Rubahn, Horst-Günter; Bozhevolnyi, Sergey I.

Published in:
Optics Express

DOI:
[10.1364/OE.19.015155](https://doi.org/10.1364/OE.19.015155)

Publication date:
2011

Document Version
Submitted manuscript

[Link to publication](#)

Citation for published version (APA):

Radko, I., Fiutowski, J., Tavares, L., Rubahn, H-G., & Bozhevolnyi, S. I. (2011). Organic nanofiber-loaded surface plasmon-polariton waveguides. *Optics Express*, 19(16), 15155-15161. DOI: 10.1364/OE.19.015155

General rights

Copyright and moral rights for the publications made accessible in the public portal are retained by the authors and/or other copyright owners and it is a condition of accessing publications that users recognise and abide by the legal requirements associated with these rights.

- Users may download and print one copy of any publication from the public portal for the purpose of private study or research.
- You may not further distribute the material or use it for any profit-making activity or commercial gain
- You may freely distribute the URL identifying the publication in the public portal ?

Take down policy

If you believe that this document breaches copyright please contact us providing details, and we will remove access to the work immediately and investigate your claim.

Organic nanofiber-loaded surface plasmon-polariton waveguides

Ilya P. Radko,^{1,*} Jacek Fiutowski,² Luciana Tavares,²
Horst-Günter Rubahn,² and Sergey I. Bozhevolnyi¹

¹*Institute of Technology and Innovation, University of Southern Denmark, Niels Bohrs Allé 1,
DK-5230 Odense M, Denmark*

²*NanoSyd, Mads Clausen Institute, University of Southern Denmark, Alsion 2, DK-6400
Sønderborg, Denmark*

[*ilir@iti.sdu.dk](mailto:ilir@iti.sdu.dk)

Abstract: We demonstrate the use of organic nanofibers, composed of self-assembled organic molecules, as a dielectric medium for dielectric-loaded surface plasmon polariton waveguides at near-infrared wavelengths. We successfully exploit a metallic grating coupler to excite the waveguiding mode and characterize dispersion properties of such waveguides using leakage-radiation microscopy.

© 2011 Optical Society of America

OCIS codes: (240.6680) Surface plasmons; (230.7380) Waveguides, channeled; (250.5300) Photonic integrated circuits; (130.5460) Polymer waveguides.

References and links

1. S. A. Maier, *Plasmonics: Fundamentals and Applications* (Springer, 2007).
2. S. Lal, S. Link, and N. J. Halas, "Nano-optics from sensing to waveguiding," *Nat. Photonics* **1**, 641–648 (2007).
3. J. N. Anker, W. P. Hall, O. Lyandres, N. C. Shah, J. Zhao, and R. P. Van Duyne, "Biosensing with plasmonic nanosensors," *Nat. Mater.* **7**, 442–453 (2008).
4. D. K. Gramotnev and S. I. Bozhevolnyi, "Plasmonics beyond the diffraction limit," *Nat. Photonics* **4**, 83–91 (2010).
5. E. Verhagen, M. Spasenović, A. Polman, and L. K. Kuipers, "Nanowire plasmon excitation by adiabatic mode transformation," *Phys. Rev. Lett.* **102**, 203904 (2009).
6. A. L. Pyayt, B. Wiley, Y. Xia, A. Chen, and L. Dalton, "Integration of photonic and silver nanowire plasmonic waveguides," *Nat. Nanotechnol.* **3**, 660–665 (2008).
7. S. I. Bozhevolnyi, V. S. Volkov, E. Devaux, J.-Y. Laluet, and T. W. Ebbesen, "Channel plasmon subwavelength waveguide components including interferometers and ring resonators," *Nature* **440**, 508–511 (2006).
8. C. Reinhardt, S. Passinger, B. N. Chichkov, C. Marquart, I. P. Radko, and S. I. Bozhevolnyi, "Laser-fabricated dielectric optical components for surface plasmon polaritons," *Opt. Lett.* **31**, 1307–1309 (2006).
9. B. Steinberger, A. Hohenau, H. Ditlbacher, A. L. Stepanov, A. Drezet, F. R. Aussenegg, A. Leitner, and J. R. Krenn, "Dielectric stripes on gold as surface plasmon waveguides," *Appl. Phys. Lett.* **88**, 094104 (2006).
10. T. Holmgaard, and S. I. Bozhevolnyi, "Theoretical analysis of dielectric-loaded surface plasmon-polariton waveguides," *Phys. Rev. B* **75**, 245405 (2007).
11. A. V. Krasavin, and A. V. Zayats, "Passive photonic elements based on dielectric-loaded surface plasmon polariton waveguides," *Appl. Phys. Lett.* **90**, 211101 (2007).
12. J. Granddier, G. C. des Francs, S. Massenot, A. Bouhelier, L. Markey, J.-C. Weeber, C. Finot, and A. Dereux, "Gain-assisted propagation in a plasmonic waveguide at telecom wavelength," *Nano Lett.* **9**, 2935–2939 (2009).
13. T. Holmgaard, Z. Chen, S. I. Bozhevolnyi, L. Markey, A. Dereux, A. V. Krasavin, and A. V. Zayats, "Wavelength selection by dielectric-loaded plasmonic components," *Appl. Phys. Lett.* **94**, 051111 (2009).
14. J. Gosciniak, S. I. Bozhevolnyi, T. B. Andersen, V. S. Volkov, J. Kjelstrup-Hansen, L. Markey, and A. Dereux, "Thermo-optic control of dielectric-loaded plasmonic waveguide components," *Opt. Express* **18**, 1207–1216 (2010).
15. J. Gosciniak, V. S. Volkov, S. I. Bozhevolnyi, L. Markey, S. Massenot, and A. Dereux, "Fiber-coupled dielectric-loaded plasmonic waveguides," *Opt. Express* **18**, 5314–5319 (2010).

16. I. P. Radko, M. G. Nielsen, O. Albrektsen, and S. I. Bozhevolnyi, "Stimulated emission of surface plasmon polaritons by lead-sulphide quantum dots at near infra-red wavelengths," *Opt. Express* **18**, 18633–18641 (2010).
17. A. H. Yuwono, B. Liu, J. Xue, J. Wang, H. I. Elim, W. Ji, Y. Li, and T. J. White, "Controlling the crystallinity and nonlinear optical properties of transparent TiO₂/PMMA nanohybrids," *J. Mater. Chem.* **14**, 2978–2987 (2004).
18. F. D'Amore, M. Lanata, S. M. Pietralunga, M. C. Gallazzi, and G. Zerbi, "Enhancement of PMMA nonlinear optical properties by means of a quinoid molecule," *Opt. Mater.* **24**, 661–665 (2004).
19. B. Kulyk, B. Sahraoui, O. Krupka, V. Kapustianyk, V. Rudyk, E. Berdowska, S. Tkaczyk, and I. Kityk, "Linear and nonlinear optical properties of ZnO/PMMA nanocomposite films," *J. Appl. Phys.* **106**, 093102 (2009).
20. F. Balzer, V. G. Bordo, A. C. Simonsen, and H.-G. Rubahn, "Optical waveguiding in individual nanometer-scale organic fibers," *Phys. Rev. B* **67**, 115408 (2003).
21. J. Brewer, C. Maibohm, L. Jozefowski, L. Bagatolli, and H.-G. Rubahn, "A 3D view on free-floating, space-fixed and surface-bound para-phenylene nanofibres," *Nanotechnology* **16**, 2396–2401 (2005).
22. K. Al-Shamery, H.-G. Rubahn, and H. Sitter, eds., *Organic Nanostructures for Next-Generation Devices* (Springer, 2008).
23. M. Schiek, F. Balzer, B. Brewer, K. Al-Shamery, and H.-G. Rubahn, "Organic molecular nanotechnology," *SMALL* **4**, 176–181 (2008).
24. J. Brewer, M. Schiek, A. Lutzen, K. Al-Shamery, and H.-G. Rubahn, "Nanofiber frequency doublers," *Nano Lett.* **6**, 2656–2659 (2006).
25. L. Tavares, J. Kjelstrup-Hansen, and H.-G. Rubahn, "Efficient roll-on transfer technique for well-aligned organic nanofibers," *Small* (2011), doi: 10.1002/sml.201100660.
26. A. Drezet, A. Hohenau, A. L. Stepanov, H. Ditlbacher, B. Steinberger, N. Galler, F. R. Aussenegg, A. Leitner, and J. R. Krenn, "How to erase surface plasmon fringes," *Appl. Phys. Lett.* **89**, 091117 (2006).
27. I. P. Radko, S. I. Bozhevolnyi, G. Brucoli, L. Martín-Moreno, F. J. García-Vidal, and A. Boltasseva, "Efficient unidirectional ridge excitation of surface plasmons," *Opt. Express* **17**, 7228–7232 (2009).
28. E. D. Palik, *Handbook of Optical Constants of Solids* (Academic, 1985).
29. A. Niko, S. Tasch, F. Meghdadi, C. Brandstatter, and G. Leising, "Red-green-blue emission of parahexaphenyl devices with color-converting media," *J. Appl. Phys.* **82**, 4177–4182 (1997).
30. J. Grandidier, S. Massenot, G. Colas des Francs, A. Bouhelier, J.-C. Weeber, L. Markey, A. Dereux, J. Renger, M. U. González, and R. Quidant, "Dielectric-loaded surface plasmon polariton waveguides: Figures of merit and mode characterization by image and Fourier plane leakage microscopy," *Phys. Rev. B* **78**, 245419 (2008).

1. Introduction

Surface plasmon polaritons (SPPs), which are surface electromagnetic waves propagating along a metal-dielectric interface [1], have been attracting much efforts during the last decade due to their great potential for development of ultracompact photonic circuits and sensors [1–4]. Among other devices, a number of SPP-based waveguiding configurations have been suggested including metal nanostripes [5] and nanowires [6] as well as V-grooves cut in metal surfaces [7]. An alternative and technologically simple strategy for achieving tight SPP mode confinement exploits the dependence of the SPP propagation constant on the dielectric refractive index (at a metal-dielectric interface) by depositing narrow dielectric ridges on the metal surface [8, 9]. The resulting configuration, known as dielectric-loaded SPP waveguides (DLSPWs) [10], has proved to be suitable for realization of passive and active plasmonic components [11–14].

A commonly used dielectric material for DLSPWs is polymethyl-methacrylate (PMMA) naturally compatible with industrial fabrication using large-scale UV lithography and allowing integration with fiber optics [15]. Thus PMMA has been widely used, since it is easy to operate with and one can modify its optical properties by embedding various molecules and nanocomposites. For instance, one can make the medium optically active, providing hereby possibilities to amplify the SPP mode [12, 16] or to introduce nonlinearity [17–19]. There are, however, alternative materials with inherent tailorable nonlinear optical and optoelectronic properties. With respect to DLSPW application, we investigate here organic nanofibers (ONFs) composed of self-assembled para-hexaphenyl (*p*6P) molecules, which exhibit optical waveguiding [20], large quantum yield, and a highly anisotropic and polarized fluorescence emission [21, 22]. If one modifies the molecular building blocks via synthetic chemistry [23], strong second-harmonic generation is observed [24]. Having typical dimensions of a few hundred nanometers width and a few tens of nanometers height, they are good candidates as the dielectric medium in

DLSPWs.

2. Fabrication of organic nanofibers and grating couplers

The ONFs were grown under high-vacuum conditions by molecular-beam epitaxy of organic molecules onto a cleaved muscovite mica substrate at the surface temperature of 440 °K (Fig. 1a). Afterwards they were transferred onto a gold surface with specifically designed grating couplers (see below), which facilitate excitation of DLSPW modes (Fig. 1b). It has been recently demonstrated in detail [25] that an easy fabrication of a large number of samples without damaging the morphology and optical properties of fragile ONFs can be achieved with a fast and large-scale transfer of nanofibers from the growing to the receiving substrate. As a result of this process, a group of well oriented and mutually parallel ONFs of up to several hundreds of micrometers length are placed close to or on predefined structures on the receiving substrate. Note that besides the morphological dimensions of individual nanofibers, also their mutual distances can be varied by varying the initial growth parameters. That way samples with long, sparse ONFs can be fabricated, which are necessary for the plasmonic loading experiments described here.

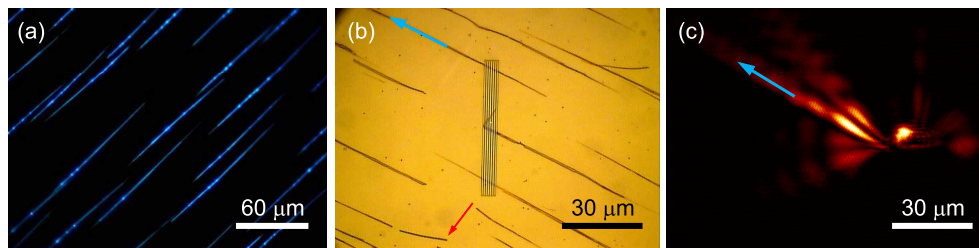


Fig. 1. (a) Epifluorescence microscopy image obtained by illuminating the sample normally with a Hg lamp at a wavelength of 360 nm. (b) Microscope image of organic nanofibers (ONFs) transferred onto a gold surface with ridge couplers (see details in text), which facilitate excitation of a DLSPW mode. (c) Leakage-radiation microscopy (LRM) image of a DLSPW mode propagating along an ONF marked with a blue arrow in the panel (b). The image is filtered in the Fourier plane [26] to remove most of the substantially brighter background, produced by SPPs, keeping the image of the DLSPW mode untouched. A more divergent beam above the DLSPW mode is a SPP excited on the grating and reflected thereafter upwards by the nanofiber. This beam has not been filtered out, because it lies very close to the DLSPW mode in the Fourier plane.

In order to excite a DLSPW mode propagating along an ONF, several periodic arrays of gold ridges were fabricated on top of a gold surface using electron-beam lithography, metal deposition, and subsequent lift-off. Such structures are known to provide high-efficiency excitation of SPPs (virtually up to 45% [27]). They are exploited here to facilitate excitation of a DLSPW mode by trying to excite a SPP at the place of overlapping of one of the ONFs with the ridge array. The grating is illuminated normally with a focused laser beam. The geometry of ridges and their period are optimized [27] for the excitation wavelength range around 800 nm: ridge height – 125 nm, ridge width – 350 nm, period – 800 nm. If the polarization of the incident light is correct (i.e., oriented across the ridges), it is easy to achieve the proper field distribution of high intensity near the ridges, which then participates in the formation of the desired waveguiding mode (Fig. 1c). During fabrication, we aimed at transferring the ONFs onto the gold surface with grating couplers so that the fibers lie perpendicular to the ridges. However, small deviations from this orientation are not critical and finally turned out to be useful to easier distinguish between the SPP and DLSPW modes, since the direction of SPP propagation in

such a configuration is essentially perpendicular to the gold ridges.

3. DLSPW modes in nanofibers

Dispersion properties of DLSPWs are well studied [10] and, besides the metal used, depend crucially on refractive index and dimensions of the dielectric part of the waveguide. We support our experimental observations with numerical evaluations of the effective index (EI) of the guided mode. In simulations, we consider a three-layer structure (glass-gold-air) with an ONF having a rectangular cross-section lying on the gold surface (Fig. 2a). Dielectric constants of gold and *p*6P are taken from [28] and [29], respectively. In order to obtain the lateral dimensions of an ONF under investigation, we perform atomic-force microscopy (AFM) scans of each nanofiber (Fig. 2b) and take cross-sections. Since the transfer of nanofibers during the fabrication process involves a stamping procedure, the resulting ONFs end up being compressed by about 20 percent (Fig. 2c).

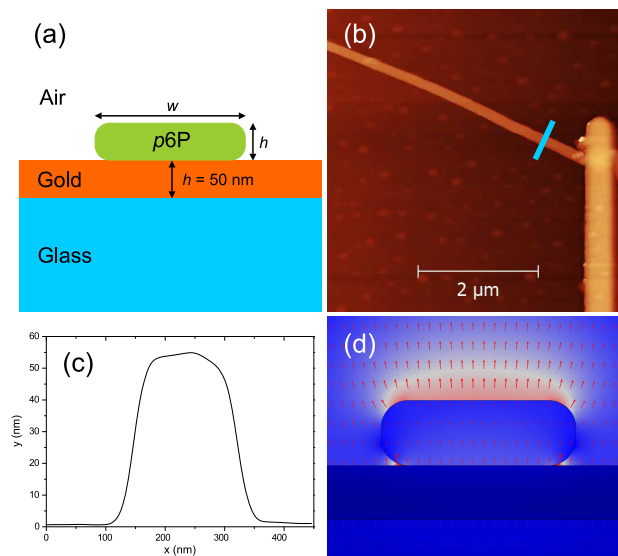


Fig. 2. (a) Geometry used in numerical evaluations of DLSPW effective index and of electric-field distribution. (b) Atomic-force microscopy (AFM) image of the ONF shown in Fig. 1b. The last ridge of the grating coupler is also visible. (c) Profile taken across the nanofiber as indicated with a blue line in the panel (b). The corresponding extracted dimensions are: $w = 180$ nm, $h = 60$ nm. The profile has a shape reminding a Gaussian due to the convolution with the shape of the AFM probe. (d) Calculated electric-field distribution of the fundamental TM_{00} mode of the DLSPW formed by the given ONF.

A field distribution of the fundamental TM_{00} mode of a DLSPW is calculated (Fig. 2d) for a particular ONF with dimensions (see Fig. 2a for definitions) $w = 180$ nm, $h = 60$ nm, and an excitation wavelength $\lambda = 800$ nm using the finite-element method (FEM). Note that even though the corners of the dielectric rectangle have been rounded ($r = 25$ nm) for the sake of higher similarity with the experiment, this is actually not required to obtain correct values of the EI of the mode, since it gives only a minor correction, typically well below the precision with which the dielectric constants of the participating materials are known.

4. Leakage-radiation microscopy characterization of organic nanofibers

We start with the investigation of the dispersion properties of ONFs using leakage-radiation microscopy (LRM). Besides direct real-time observation of SPPs, this technique allows for quantitative Fourier-plane characterization of DLSPW modes, namely one can prove the mere existence of a waveguiding mode and find its EI [30]. The presence of a straight line in the Fourier image (i.e., a line in the k -vector space) is an indication of a mode that has a fixed component of its k vector, directed perpendicular to that line, and a widely varying component of the k vector (i.e., an undefined value) in the perpendicular direction. The former direction is along the waveguide, and the corresponding component of the k vector is the k vector of the mode, whereas the latter direction is across the waveguide, and the largely varying component of the k vector is due to a tight transversal confinement.

We characterize the dispersion properties of an ONF shown in Fig. 3a, which has the width $w = 190$ nm and the height $h = 44$ nm. The line corresponding to the DLSPW mode features slight displacement in the Fourier-space images obtained at different wavelengths (Figs. 3b and 3c). By taking a cross-section *at exactly the same place* in the Fourier images and comparing them versus each other (Fig. 3d), we evaluate the dispersion of the mode EI and compare that with values obtained numerically using FEM and the effective-index method (EIM) [10].

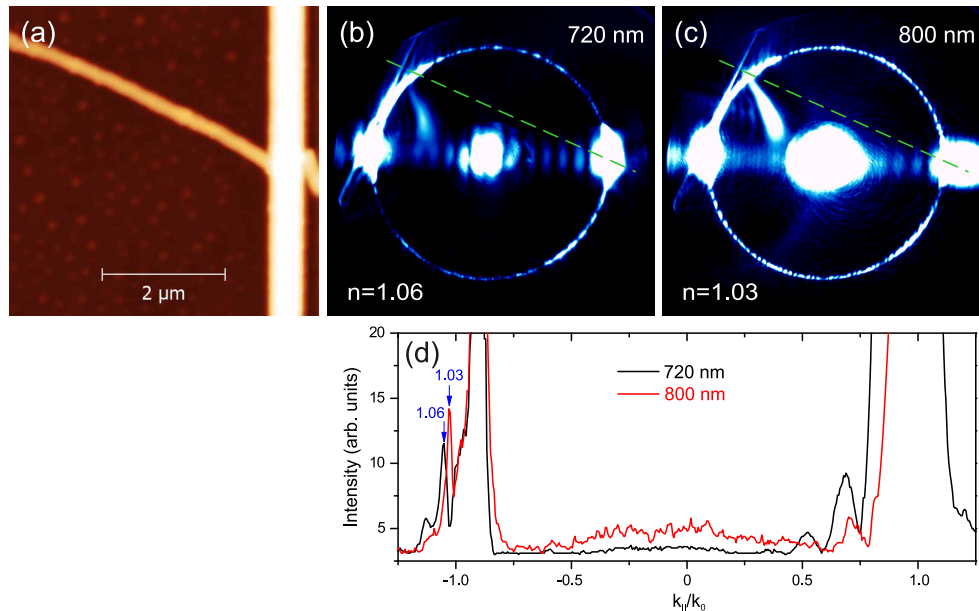


Fig. 3. (a) AFM image of an ONF whose dispersion properties have been investigated. The last ridge of the grating coupler is also visible. (b), (c) LRM images of the DLSPW mode propagating along the ONF shown in panel (a) taken in the Fourier plane. The excitation wavelength is (b) 720 nm and (c) 800 nm. The guided mode is represented with a straight line. The circle touching the line corresponds to a SPP at the gold-air interface. (d) Profiles taken across the Fourier images along the dashed lines in panels (b) and (c). A tiny displacement of the maximum corresponding to the DLSPW mode indicates a change of the mode effective index.

The absolute values of the EI obtained experimentally have relatively large errors, comparable to the value of the dispersion (Table 1). The shift of the EI with the wavelength is obtained quite precisely though, and is in very good agreement with the numerical simulations. One can

also notice that the much simpler EIM gives the results very similar to FEM, which was already observed previously [10].

Table 1. Evaluated DLSPPW Mode EI for the ONF Shown in Fig. 3a*

λ , nm	Experiment	FEM	EIM
720	1.06 ± 0.02	1.066	1.057
760	1.05 ± 0.02	1.043	1.041
800	1.03 ± 0.02	1.029	1.031
850	1.02 ± 0.02	1.017	1.023

*The dimensions of the ONF (see. Fig. 2a for definitions): $w = 190$ nm, $h = 44$ nm.

We demonstrate the advantage of using grating couplers to excite DLSPPW modes in ONFs by showing the possibility to excite modes in nearby nanofibers (Fig. 4a) through SPPs rather than through direct illumination of ONFs. Even though the second ONF lies approximately $5 \mu\text{m}$ away from the grating and hence is not illuminated with a laser beam upon excitation, its mode is excited as efficiently as the mode of the first ONF, which is evidenced by the Fourier image (Fig. 4b).

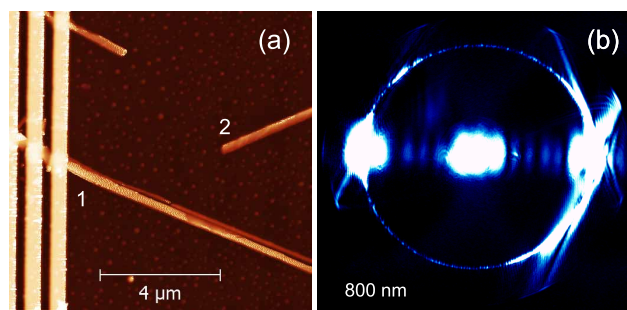


Fig. 4. (a) AFM image of three ONFs in close proximity to each other and (b) the corresponding LRM image taken in the Fourier plane. The excitation wavelength is 800 nm. The two DLSPPW modes of ONFs 1 and 2 are visible from the right side of the circle. The mode on the left side of the circle is the counter-propagating DLSPPW mode of the ONF 1 from the other side of the grating [not visible in panel (a)].

This is opposed to the case of a separated ONF (Fig. 5a) whose mode can be excited only upon direct illumination with a laser beam. Judging from the intensity of the DLSPPW line in the Fourier plane (Fig. 5b), we conclude that the corresponding excitation efficiency is substantially smaller. Note that the SPP excitation is weaker as well since the ONF is very wide and low in height ($w = 530$ nm, $h = 40$ nm), which is far from the optimum geometry for this wavelength [27].

5. Conclusion

In summary, we have demonstrated the possibility to use organic nanofibers (ONFs), composed of self-assembled oligomer para-hexaphenyl (*p6P*) molecules, as a dielectric medium for DLSPPW. ONFs can be fabricated from organic molecules with large hyperpolarizabilities and thus will show strong nonlinear properties, providing hereby access to the realization of active all-optic plasmonic devices. We have characterized the dispersion properties of a chosen waveguide both experimentally using leakage-radiation microscopy and numerically using finite-element and effective-index methods. The obtained values of the effective mode index of

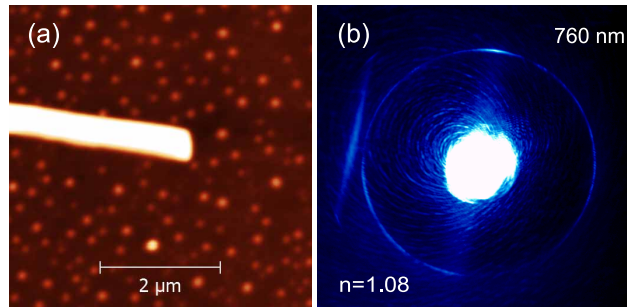


Fig. 5. (a) AFM image of a separated ONF marked with a red arrow in Fig. 1b and (b) the corresponding LRM image taken in the Fourier plane. The excitation wavelength is 760 nm.

the waveguide are in good agreement between all three methods used. We demonstrated also an advantage of using a grating coupler to facilitate excitation of the DLSPW mode in organic-nanofiber-loaded waveguides. While the grating-assisted excitation of ONF-based DLSPWs is useful for further investigations of this promising plasmonic configuration, a more robust coupling approach, e.g. by using optical fibers [15], should be developed in order to bring it closer to practical applications. This is a very challenging task that will be addressed in our future research.

Acknowledgments

This work was supported by the Danish Council for Independent Research (FTP-project No. 09-072949 ANAP). We are grateful to Jakob Kjelstrup-Hansen and Kasper Thilising-Hansen for invaluable support in preparing organic nanofibers and structured plasmonic samples.